Title	Towards the Use of High Strength Steel for Construction Productivity
Author(s)	Chiew, Sing Ping; Zhao, Mingshan; Cai, Yanqing
Citation	Chiew, S. P., Zhao, M., & Cai, Y. (2016). Towards the Use of High Strength Steel for Construction Productivity. Australasian Structural Engineering Conference: ASEC 2016.
Date	2016
URL	http://hdl.handle.net/10220/42780
Rights	© 2016 Engineers Australia. This is the author created version of a work that has been peer reviewed and accepted for publication by Australasian Structural Engineering Conference: ASEC 2016, Engineers Australia. It incorporates referee’s comments but changes resulting from the publishing process, such as copyediting, structural formatting, may not be reflected in this document.

Towards the Use of High Strength Steel for Construction Productivity

<u>S.P. Chiew</u>, M.S. Zhao and Y.Q. Cai*
School of Civil and Environmental Engineering
Nanyang Technological University, Singapore
*(*Email: cspchiew@ntu.edu.sg)*

ABSTRACT

With rapid advancement in on-line steel production processes, it is now possible to produce high strength steel at affordable and competitive cost. This leads to the development of design codes and construction technologies where higher strength and performance steel are now permitted to be used. Due to its higher strength to weight ratio, saving in total materials and easier construction, higher productivity could be achieved by replacing normal strength steel with high strength steel in design and construction. However, there are key differences between high strength and traditional normal strength steel because of the way it is produced as well as limiting design considerations which will impede greater usage of high strength steel. This paper discusses the novelty as well as challenges of using high strength steel to improve construction productivity. The study of the tensile behavior of Grade S690 T-stub joints is highlighted to illustrate the difference between high strength and normal strength structural steel. The design issues of using high strength Grade 600 reinforcing steel bars and high strength steel in composite columns are also highlighted.

Keywords
High strength steel; construction productivity; structural steel; reinforcing steel; composite steel

1. INTRODUCTION

Steel is one of the most successful civil engineering materials in construction due to its high strength, stiffness, toughness and ductile properties. With latest and innovative developments in the manufacturing and production processes, the material has undergone significant changes. For example, in the 1900s, the primary structural steel had nominal yield strength of about 220MPa, which by today's standard, is referred to only as mild steel. The once so-called "high strength" steel S355 is a commonly used structural steel grade and steel with yield strength lower than 460MPa have been commonly specified for applications in many structural design codes (AISC 2005; BSI 2005). The interests today are in high strength steel (HSS) over normal strength steel (NSS) because of the recognition of the benefits in higher strength to weight ratio, lower cost in total materials and aesthetic advantages. This kind of steel is usually manufactured from soft and ductile steel with yield strength less than 300MPa by some sort of combined thermo-mechanical rolling, quenching and tempering techniques and is often denoted as quenched and tempered (QT) or thermo-mechanical controlled process (TMCP) steel and they are most often found in the form of steel plates.

However, strength is not the only aspect that HSS differs from the traditional normal strength steel (NSS). One major issue against the popularization of HSS is that the quenching and tempering process improves the strength at the expense of ductility through complicated heat treatments. Massive researches have demonstrated that it is not possible for QT steel to achieve good deformation capacity (Bjorhovde 2004; Girão Coelho and Bijlaard 2007; Uy 2008) and they are more susceptible to heat (Chen and Young 2006; Qiang, Bijlaard et al. 2012) than mild steel, as inherited from the heat-treatment hardened microstructures (Bhadeshia and Honeycombe 2006). Nevertheless, despite the large number of reports claiming the existence of welding issues (high residual stress level and HAZ property alternation) in HSS, few works regarding the effects of these issues on the performance of HSS structures can be found in literature, let alone the recommendations and cautions given for designing or evaluating the performance of HSS structures. In this paper, the possibility of extending the usage of HSS in construction is discussed. Highlights are given to the tensile behavior of T-stub joints made of high strength structural steel in Grade S690, and the issues of using high strength reinforcing steel Grade 600 bars and high strength steel in composite steel-concrete column members.

2. HIGH STRENGTH STEEL AND CONSTRUCTION PRODUCTIVITY

In EC3, a structural steel can be classified as HSS given that $460 < \mathrm{f_y} < 700$MPa, $\mathrm{f_u}/\mathrm{f_y} \geq 1.05$, elongation at failure not less than 10%, and $\varepsilon_u \geq 15\varepsilon_y$, while the rest mechanical properties remain the same as NSS (BSI 2005). For a typical type of quenched and tempered steel S690Q, the actual yield strength can be twice as much as that of NSS S355. This means that for the same amount of strengths provided by S690 and S355, using S690 saves 50% of the material for S355. In the meantime, the structural weight, construction and transportation difficulties can be greatly reduced. What is more, smaller size of the structure is definitely favorable in the view of design and aesthetic appearance. In short, as far as improving construction productivity is concerned, steel with higher strength are the answers.

In the UK, the use of high strength steel can be traced back to the early 1970s when the Grade X70 (460MPa) was introduced as line pipe for gas transmission (Bai and Bai 2014). Following the successful experience gained with X70, higher Grade X80 with yield strength more than 550MPa is becoming common. Later, the Hutton Field floating structure which is a tension-leg platform used steel with a minimum yield strength of 795MPa (Pocock 2006). A survey taken in 1995 indicted that the proportion of high strength steel used in offshore structures increased from less than 10% to over 40% over time less than a decade (Healy and Billingham 1995). One of the major advantages of using high strength steel in off-shore structures comes from the potential to greatly reduce the section size and weight. Although high strength steel are more commonly used in offshore structures, building designers have long been aware of the possibility and potential of the application of high strength steel in onshore structures. The Landmark Tower in central Yokohama, Japan used steel with a minimum tensile strength of 600MPa. Steel plates manufactured with thermo-mechanical process were fabricated into I section columns. The first use of high strength steel with yield strength above 690MPa was in Australia in 1989. The 30-story high Sydney Grosvenor Place and Perth Central Park in Perth used S690 to fabricate concrete encased and concrete filled columns. In the Start City in Sydney, S690 high strength steel was used again in both basement columns and the theater roof truss (Pocock 2006).

Essentially, steel are just alloys of iron with carbon, which may contribute up to 2.1% of its weight. Although the properties of steel are greatly affected by its chemical composition, various treatments to which the steel may be subjected after leaving the manufacturing line, can still remarkably affect the mechanical properties. One important reason for the overwhelming dominance of steel is the endless variety of microstructures that can be generated by solid-state transformation and processing. For example, the strength of an unalloyed carbon steel can be increased by up to 500% just by changing the cooling rate during austenite decomposition from extremely low to extremely fast (Tensi, Stich et al. 2007). Since many of those treatments involve the change of temperature of the steel in solid state, the term heat treatment is used to cover all those treatments. The main reason that NSS and HSS have similar chemical composition yet drastic different mechanical properties except for elastic modulus is that HSS usually goes through heat treatment hardening processes, more specifically, quenching and tempering after rolling. In modern structural steel mills, quenching is most commonly used to harden steel by introducing martensite, which grants the HSS its major mechanical properties. It should be noted that the main constitution of HSS, the martensite, is extremely hard but brittle and susceptible to heat in nature. As a result, the performance of HSS cannot get rid of these impressions easily.

To improve construction productivity, high heat input welding techniques such as submerged arc welding (SAW) and electro-slag welding (ESW) are preferred than traditional low heat input welding techniques such as flux core arc welding (FCAW) and gas-shielded/shielded metal arc welding (GMAW and SMAW). In Japan, SAW and ESW are very widely used to form prefabricated box columns in factories while GMAW and SMAW are used to finishing the connections on site. As can be seen from Figure 1, the heat input of the SAW and ESW are 25 and 40 times that of the GMAW. Since the moving speeds of the welding electrodes do not differ much, the efficiencies of these methods are similar to the heat input. However, such high efficiencies are not coming without any expense - the sizes of the heat affected zone (HAZ) of the SAW and ESW are so much bigger than those of the GMAW (Figure 1). The well-known effects of the HAZ include issues of high residual stress, mechanical property alteration, toughness loss and cold crack. Under the cases of high heat input welding, it is obviously not wise to ignore all these issues. Although HSS bars and steel for composite constructions may be different from high strength structural steel, they are usually made by the same technologies and therefore cannot escape from these problems.

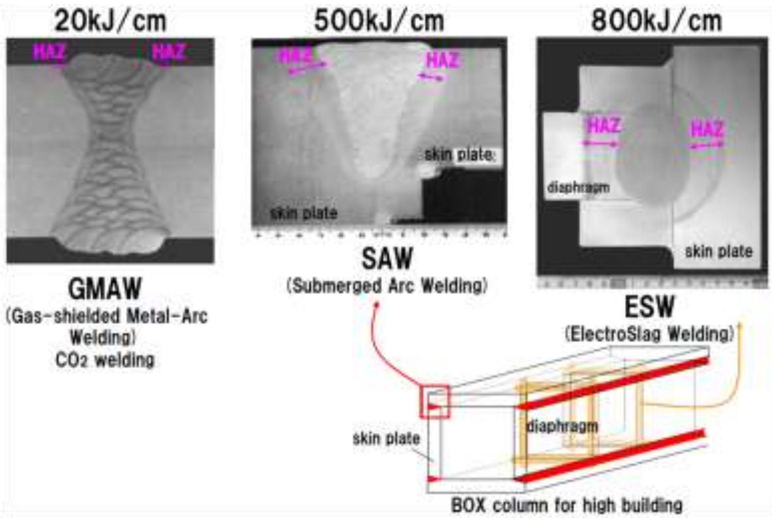

Figure 1. Common welding techniques for improving productivity

3. HIGH STRENGTH STRUCTURAL STEEL

HSS being short of deformation ability is no news, especially after affected by welding (Bjorhovde 2004; Girão Coelho and Bijlaard 2007; Uy 2008). Some reports concerning high strength steel (S460 and S690) at elevated temperatures (Chen and Young 2006; Qiang, Bijlaard et al. 2012; Qiang, Bijlaard et al. 2012; Chiew, Zhao et al. 2014) found that the deterioration of strength seemed could be more serious than that of normal strength steel, and the deterioration extents vary with steel. Extensive research also found that the mechanical properties of HSS after exposure to heat (after heated to high temperatures and cooled down) may deteriorate (Chiew, Zhao et al. 2014). Although the literature has pointed out so many disadvantages of HSS in material property aspects, the member behaviors under compression seems not to be much different from NSS (Zhao, Van Binh et al. 2004; Shi, Ban et al. 2012; Wang and Young 2013; Han, Hou et al. 2014). The possible explanation here is that when buckling is involved, the behavior is no longer dominated by strength.

For weight critical construction, using of HSS is one efficient way to save energy and to minimize the carbon foot print (Yorgun and Bayramoglu 2001). Current design codes such as EN1993-1-8 (BSI 2005) give general design methods for design of joints subject to predominantly static loading using steel Grades less than S460. EN1993-1-12 (2007) extends some design rules to cover the steel Grades up to S700. However, the rules for design structural joints in tensions not one of them. This study focuses on the tensile performance of the welded HSS connections. One of the most frequently seen connections is the equivalent T-stub joints, as shown in Figure 2.

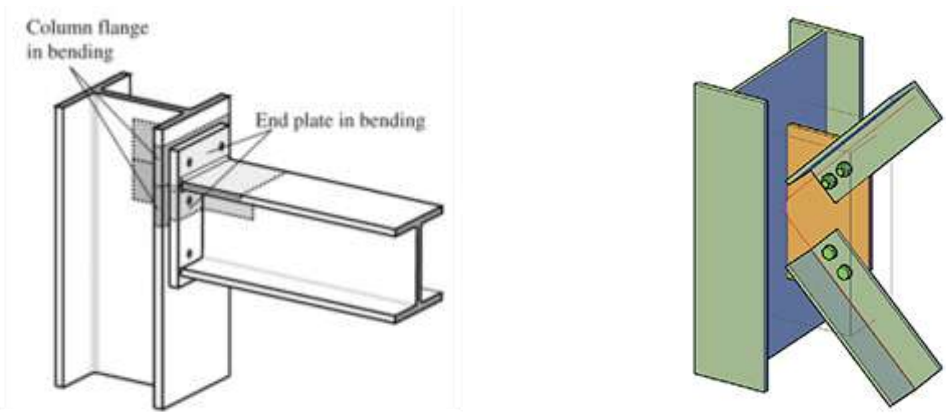

Figure 2. Beam-column connections (left) and gusset plate connections (right)

3.1 Material

Two types of materials are examined in this study: Thermal Mechanical Controlled Process Steel Plate (TMCP) in Grades S385 and S440 and Reheated, Quenched and Tempered Steel Plate (RQT) in Grade S690. Both types of materials are emerging for the structural usage in contrast to the traditional NSS S355 or mild steel S237 and S275. TMCP is an advanced thermo-mechanical process to produce low carbon plate steel. The concept of TMCP combines controlled hot rolling with accelerated cooling to control the microstructure (Nakano, Saito et al. 1988; Hasegawa, Tomita et al. 1998). RQT is essentially a refined quenching and tempering technology. RQT steel plates exhibit better homogeneity in through-thickness mechanical properties compared with traditional directly quenched and tempered steel plates. The mechanical properties of the studied materials are presented in Table 1, in comparison with the corresponding standards including EN 10025-4 (BSI 2004) and EN 10025-6 (BSI 2004) for TMCP and RQT products, respectively. From Table 1, two distinct features of RQT-S690 can be read: 1, This material has superior strengths compared to traditional steel. The actual yield strength of RQT-S690 is more than twice of the nominal yield strength of S355. 2, RQT-S690 is very brittle compared to traditional NSS or the two types of TMCP in this study. For TMCP, it can also be seen from Table 1 that the TMCP-S385 literally fulfilled the mechanical property specifications of S420M/ML and the TMCP-S440 fulfilled those of S460M/ML.

Table 1. ***Mechanical properties of RQT-S690, TMCP-S385 and TMCP-S440***

Strengths	fy (MPa)	fu (Mpa)	E (Gpa)	Elongation (%)
RQT-S690 (16mm)	745.2.0	837.8	208.9	14.5
EN 10025-6 S690Q/QL (3mm≤t≤50mm)	690	770-940	-	14
TMCP-S440 (22mm)	527.3	601.3	206.9	29.2
EN 10025-4 S460M/ML (16<t≤40mm)	440	540-720	-	17
TMCP-S385 (16mm)	443.3	568.0	208.4	37.8
EN 10025-4 S420M/ML (t≤16mm)	420	520-680	-	19

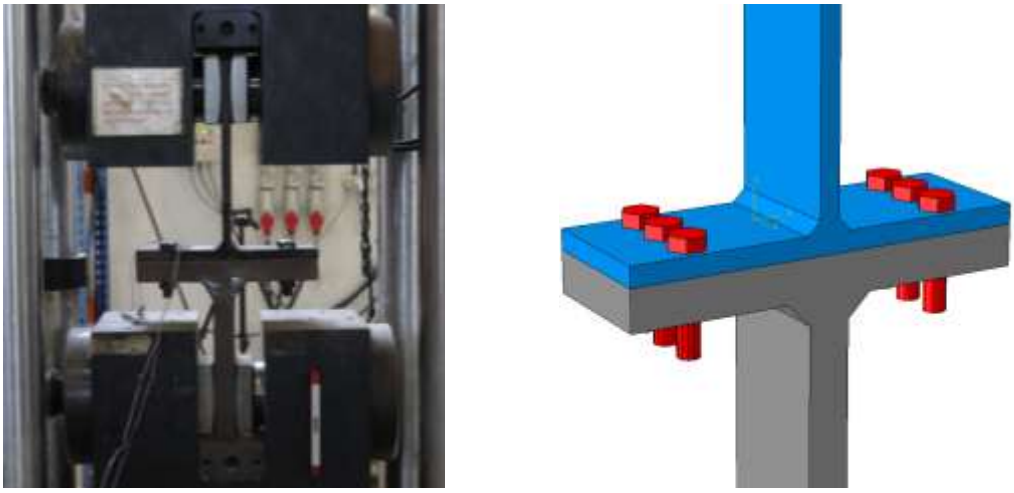

Figure 3. Tensile test setup (left) and analytical model (right)

3.2 Specimen and Test Set-up

Twelve(12) T-joints were fabricated and tested in this study. They were of the same configuration but different thicknesses and materials. Each specimen is fabricated by joining two identical sheets with dimensions of 440×150×t mm, where t is the thickness. The joints are designed as complete joint penetration butt weld according to the AWS structural steel welding code (AWS 2008). Three bolt holes were drilled at each side of the chord plate in order to fix the specimens in the test rig. The distance between two rows of bolt holes (center to center) is 290 mm. To finish the weld work, the SMAW method was employed. Compared to the other common welding methods, SMAW is more friendly to martensite-based HSS due to the low heat input (Mohandas, Madhusudan Reddy et al. 1999) which may less affect the HAZ.

The tensile tests for the RQT-S690 welded PtP joints were carried out in a servo-hydraulic universal test machine that has a maximum loading capacity of 2000KN. To fix the specimen into the test machine, support joints made of S355 steel plates with thickness of 50mm were fabricated. The specimens are fixed into the support joints by 6 high strength hexagon bolts in Grade 10.9HR, M24, as shown in Figure 3. Displacement load instead of force load was used during loading, since it would be easier to control the loading time. The loading rate was set as 1mm/min for all the specimens so that stable static response could be obtained.

3.3 Test Results
3.3.1 General Description

Figures 4 and 5 present the test results in terms of load-displacement curves of the TMCP and RQT steel T-stub joints, respectively. Despite that the specimens may fail in different modes, the curves are of the same pattern. In general, three stages in the load-displacement curves can be distinguished: (1) the elastic stage, (2) plastic hinge development stage and (3) the failure stag, as shown in Figures 4 and 5. In the elastic stage, stiffness and the elastic modulus govern the behaviors of the joints until general yielding takes place. Within this stage, the load increases rapidly with a high load / displacement ratio, which is dependent on the stiffness of the joint, more specifically, the angle and thickness. When the specimens are further loaded, plastic deformation would appear and obvious plastic hinges could be seen. The positions of the plastic hinges are almost fixed: two at near the weld toes and the other two near the bolt hole. In this stage, the deformation grows wildly but the carried load increases slowly. It is worth noting that the curves of the same angle group are generally parallel to each other. If the loads are further increased, stronger hardening effects than those in the plastic hinge development stage occur and the parallel relationship in the Load-displacement curves of each angel group disappear. In a short loading time, final failure appeared as either weld toe through thickness fracture or bolt hole necking failure.

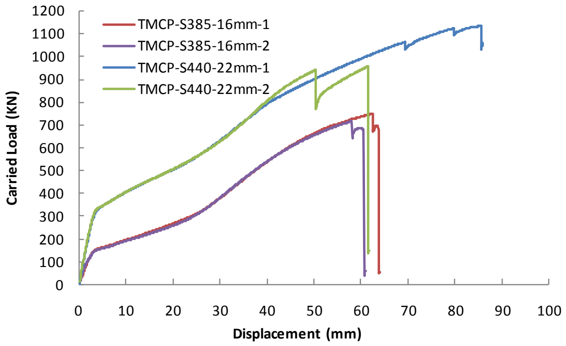

Figure 4. Load-Displacement curves of the TMCP T-stub joints

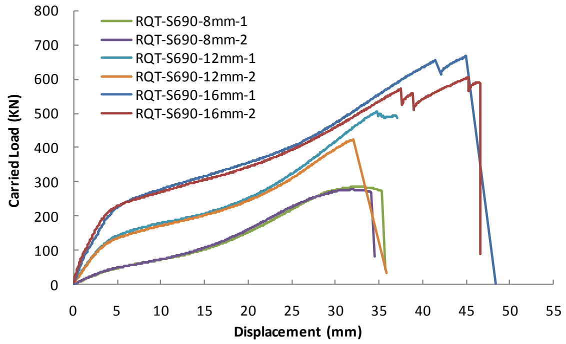

Figure 5. Load-Displacement curves of the RQT T-stub joints

Figure 6. Plastic hinge phenomena

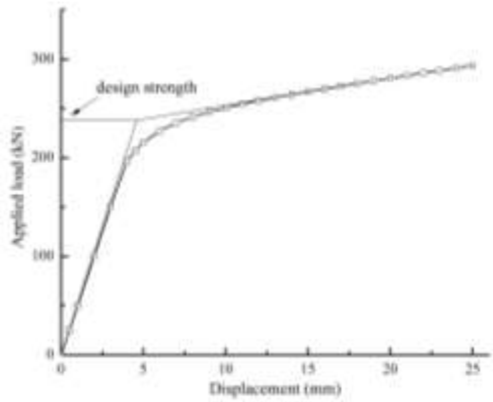

Figure 7. Simplified elastic-plastic load-displacement curve

3.3.2 Stiffness of the Elastic Stage

For design purpose, the ultimate load carrying capacity or the behavior of the joints under the elastic stage is of the most importance. From Figures 4 and 5, it can be seen that not only the stiffness but also the deformation limit of the elastic stage vary according to the configuration and material of the specimens. To quantitative evaluate these two parameters; the yield line theory is introduced. The elastic stage and plastic hinge development stage of the curves are taken out and simplified into straight line model, as shown in Figure 7. The turning point is defined as the plastic resistance, which is widely accepted as the load carrying capacity before large deformation appears (Al-Khatab and Bouchaïr 2007). Based on the simplified load-displacement model, the global stiffness of the studied T-stub joints under the elastic stages is defined as:

$$E_G = \frac{F_L}{D} \qquad \text{(Eqn. 1)}$$

where E_G is the global stiffness; F_L is the load at certain level of elastic displacement d.

The calculated stiffness for all the tested joints is shown in Figure 8. It can be seen from Figure 8 that the test results are repeatable and stable. The maximum differences between the specimens in the same configuration occurred at the RQT-S690-8 and 16mm and are only 3.2%. The stiffness in terms of carried load (KN) per displacement (mm) increases rapidly with the thickness of the specimens. The stiffness of the 16mm RQT specimens is about 5.3 times of that of the 8mm RQT specimens, while the stiffness of the TMCP-22mm is slightly less than 2 times of that of the TMCP-16mm. Besides, although the RQT-S690-16mm and the TMCP-S385-16mm had exactly the same configuration, the RQT-S690-16mm specimens show slightly higher stiffness. From Figure 8, it can be seen that the stiffness-thickness relationship is generally linear. The equation of the trend line is obtained and expressed as:

$$y=6.520x-40.98 \qquad \text{(Eqn. 2)}$$

It can be seen from Figure 8 that the trend line equation agreed well with the test results, except for the TMCP-S385-16mm. For the rest, the maximum difference is only 4.0%.

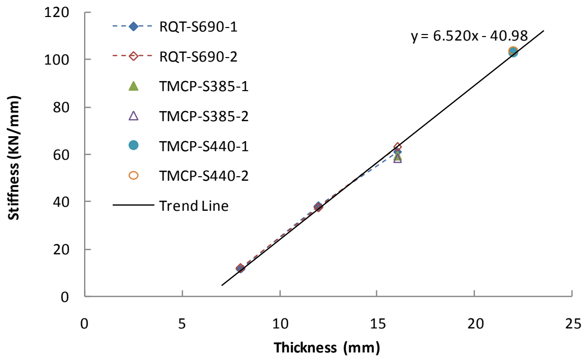

Figure 8. Stiffness of the elastic stage

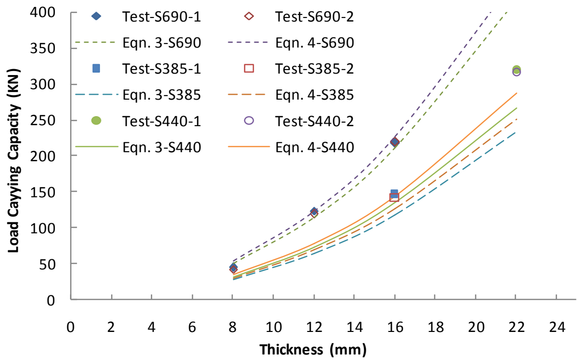

Figure 9. Load carrying capacities

3.3.3 Plastic Resistance

In EC3, there are three types of failure modes for typical T-stub joints, i.e. complete yielding of the flange, bolt failure with yielding of the flange and bolt failure (BSI 2005). In this study, all the specimens are failed in failure mode 1 and only slight plastic deformation was found in the bolts for TMCP-S440-22mm. The EN 1993-1-8 (BSI 2005) gives two methods based on yield line analysis to predict the load carrying capacity of the T-stub joints failed in complete yielding of the flange:

Method 1: $F = \frac{4M_{pl,1,Rd}}{m}$ (Eqn. 3)

Method 2: $F = \frac{(8n-2e_w)M_{pl,1,Rd}}{2mn-e_w(m+n)}$ (Eqn. 4)

where $M_{pl,1,Rd} = 0.25 l_{eff}(t)^2 f_y$ is the design moment resistance of the section, leff, m, n are geometrical parameters of the T-stub test setup; e_w is 1/4 of the washer diameter or the width across points of the bolt head of nut, as relevant. In method 2, the force applied to the T-stub flange b a bolt is assumed to be uniformly distributed under the washer, the bolt head or the nut, instead of concentrated at the center line of the bolt. This assumption leads to higher value but is more realistic, since the distance between the center lines of the weld toe plastic hinge and bolt area plastic hinge is smaller than n especially at the beginning of the plastic hinge development stage.

The load carrying capacities of the studied T-stub joints obtained by the yield line method and EC3 equations are shown in Figure 9. From Figure 9, it can be seen that the load carrying capacity of the RQT specimens are superior compared to the TMCP specimens. The average load carrying capacity of the RQT-S690-16mm is about 91.3% more than that of the TMCP-S385-16mm. However, the test results of the RQT-S690 specimens are generally below anticipation compared to the EC3 equations. The load carrying capacity of the RQT-S690-8mm is much lower than both Eqn. 3 and 4, and the RQT-S690-12mm and 16mm are only slightly higher than Eqn. 3 and lower than Eqn.4. On the contrary, the test results of the TMCP specimens are about 20% higher than the Eqn. 3 and at least 11.4% higher than the Eqn. 4. Accordingly, it seems that the load carrying capacity equations in EC3 are conservative for the TMCP-S385 and S440 but not conservative for the RQT-S690. Despite that HSS RQT-S690 has shown superior behavior in the elastic stage and plastic hinge development stages compared to TMCP-S385 and S440, the deformation capacity, or ductility, of the RQT-S690 is much worse than the TMCP materials. By the benefit from better ductility, the TMCP-S385-16mm specimens show even higher maximum carried loads than RQT-S690-16mm. This fact reveals that the ultimate strength of RQT-S690-16mm cannot be utilized as efficiently as NSS, and HSS may not be a good option in the cases that ductility or maximum strength utilization is required, e.g. earthquake.

4. HIGH STRENGTH REINFORCING STEEL

4.1 Stress-Strain Curves

The design stress-strain curves for concrete and reinforcement are defined in EN 1992-1-1 (BSI 2004). For reinforcement the code specifies the use of bi-linear stress-strain curve. In each case, it is possible to choose between two possible bi-linear diagrams for the design of sections: one with a horizontal top branch and one with an inclined top branch, as shown in Figure 10. For concrete, three possibilities are described in EN 1992-1-1, as shown in Figure 11-13. The preferred idealization is the parabolic-rectangle diagram, but a bi-linear stress-strain relation and a rectangular stress distribution are also permitted. It is universal to define failure of concrete in compression by means of a limiting compressive strain. EN 1992-1-1 adopts a limit of εcu2 (or εcu3if bi-linear relation of Figure 12 is used) for flexure and for combined bending and axial load, and a limit of εc2or εc3for axial compression.

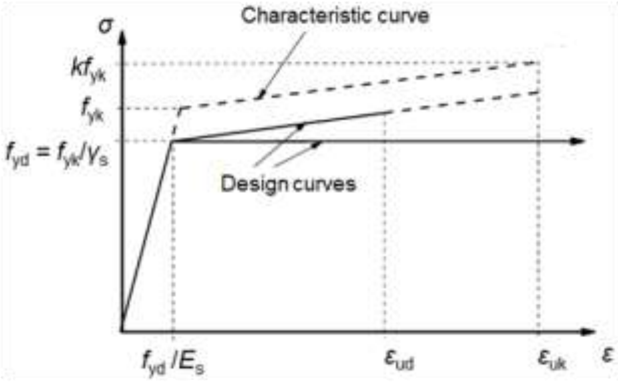

Figure 10. Stress-strain curves for reinforcing steel

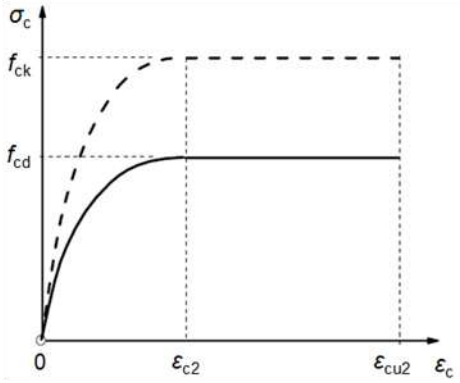

Figure 11. Parabola-rectangular diagram

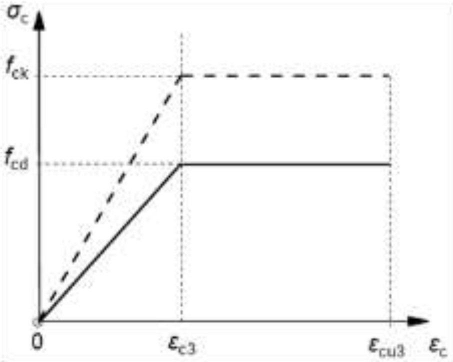

Figure 12 Bi-linear stress-strain relationship

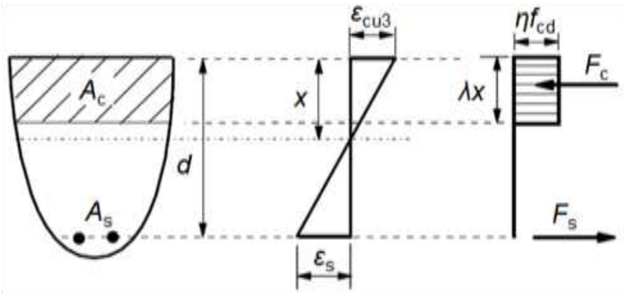

Figure 13. Rectangular stress distribution

Table 2. ***Limiting strains for concrete***

Grade	ε_{cu2} (ε_{cu3})	ε_{c2}	ε_{c3}
≤ C50/60	0.0035	0.0020	0.00175
C55/67	0.0031	0.0022	0.0018
C60/75	0.0029	0.0023	0.0019
C70/85	0.0027	0.0024	0.0020
C80/95	0.0026	0.0025	0.0022
C90/105	0.0026	0.0026	0.0023

4.2 Issues of using High Strength Grade 600 Reinforcing Bar

EN 1992-1-1 is valid for yield strength of reinforcement in the range of 400-600MPa. However, EN 1992-1-1 is mainly based on CEB Model Code for Concrete Structures which has not been checked sufficiently for use with steel yield strength higher than 500MPa. Therefore, the issue of the use of EN 1992-1-1 for Grade 600 (or higher strength) reinforcing steel still need to be studied.

The compression reinforcement in RC members has to undergo the same strain or deformation as the surrounding concrete, thus the reinforcing steel strength should be limited to the reinforcing steel stress corresponding to the limitation of the concrete compression strain (Table 2).For high strength reinforcing steel, the stress at the limiting strains may lower than its yield strength, as shown in Figure 14. It means that the maximum stress in the reinforcing steel that can be developed is also limited by those strains. Therefore, for high strength reinforcing steel in compression, it is necessary to ensure that yielding of the reinforcing steel occurs before the concrete reaches its maximum strain. Hence, the maximum strength of reinforcing steel at the maximum compression strain of concrete may be calculated with the elastic modulus of the reinforcing steel E_s = 200GPa

.

Table 2 shows the maximum strength of Grade 600 reinforcing bars corresponding to the compression strain of concrete. It can be found that the full strength of Grade 600 steel bars is generally available for compression reinforcement to resist bending or combined bending and axial compression. However, the full strength of Grade 600 steel bars is not available for compression reinforcement to resist axial compression. Therefore, the engineers should stay a bit more conservative in designing for compression reinforcement of Grade 600 steel bars or higher in order to use it with sufficient safety factor.

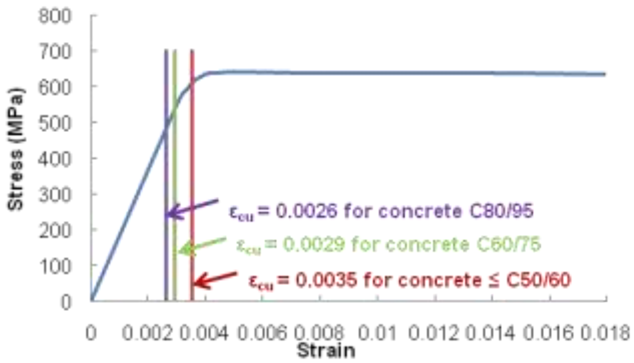

Figure 14. Stress – strain curve of Grade 600 bar

Table 3. ***Maximum strength of Grade***

Grade	$f_{y,\varepsilon_{cu}}$	$f_{y,\varepsilon_{c2}}$	$f_{y,\varepsilon_{c3}}$
≤ C50/60	600	460	403
C55/67	600	506	414
C60/75	600	529	437
C70/85	600	552	460
C80/95	598	575	506
C90/105	598	598	529
$f_{y,\varepsilon_{cu}} = E_s \varepsilon_{cu} \gamma_s \le f_{yk}$			

4.3 Effect of Confined Concrete on High Strength Grade 600 Bars

The confinement of concrete by suitable arrangements of transverse reinforcement results in a significant increase in both the strength and the ductility of compresses concrete. In the absence of more precise data, the stress-strain relation of confined concrete shown in Figure 15 may be used, with increased characteristic strength and strains according to:

$$f_{ck,c} = f_{ck}\left(1.0 + 5.0\sigma_2 / f_{ck}\right) \quad \text{for} \quad \sigma_2 \le 0.05 f_{ck}$$
$$f_{ck,c} = f_{ck}\left(1.125 + 2.5\sigma_2 / f_{ck}\right) \quad \text{for} \quad \sigma_2 > 0.05 f_{ck}$$
$$\varepsilon_{c2,c} = \varepsilon_{c2}\left(f_{ck,c} / f_{ck}\right)^2$$
$$\varepsilon_{cu2,c} = \varepsilon_{cu2} + 0.2\sigma_2 / f_{ck} \qquad \text{(Eqn.5)}$$

where σ_2 is the effective lateral compressive stress at the ULS due to confinement.

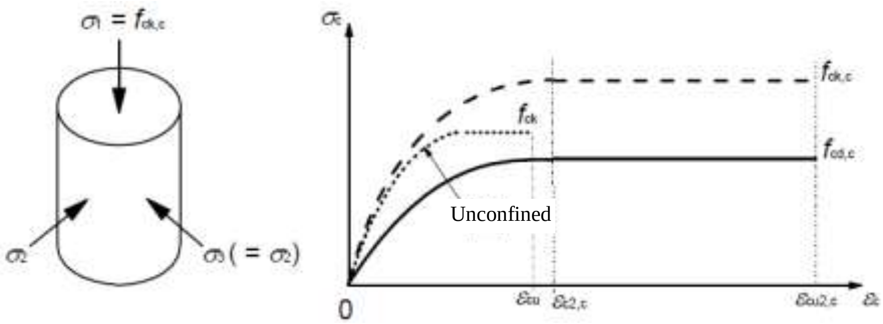

Figure 15. stress-strain relationship for confined concrete

According to CEB Model Code, simplified models may be used for the evaluation of σ_2.

$$\sigma_2 / f_{ck} = 0.5\alpha\omega_{wd} \qquad \text{(Eqn.6)}$$

with $$\omega_{wd} = \frac{W_{s,trans}}{W_{c,cf}} \frac{f_{yd,trans}}{f_{cd}}$$

$$\alpha = \alpha_n \alpha_s = \left(1 - \frac{8}{3n}\right)\left(1 + 0.5\frac{s}{b_0}\right)$$

,where ω_{wd} is the design mechanical volumetric ration of confining reinforcement, $W_{s,trans}$ is the volume of closed stirrups or cross-ties, $W_{c,cf}$ is the volume of confined concrete, $f_{yd,trans}$ is the design strength of transverse reinforcement, f_{cd} is the design strength of unconfined concrete, α is the effectiveness of confinement taking account of the non- uniformity of distribution of confining stress, α_n depends on the arrangement of hoops in the cross-section, n is the number of tied longitudinal bar, α_s depends on the spacing of hoops, sis the spacing of transverse reinforcement, b0is the width of the confined concrete.

The increased strain $\varepsilon_{c2,c}$ of confined concrete can be calculated based on Eqn.5 and Eqn.6. The results are shown in Figure 16. It can be found that the strain has a significant increased due to confinement. With the increased compression strain, the maximum stress of high strength reinforcing bar Grade 600 used in column under axial compression is also increased accordingly. The full strength of Grade 600 reinforcing bar is available when the ratio of σ_2/f_{ck} reaches a certain value, as shown in Table 4.Therefore, confined concrete generated by adequately closed links or cross-ties make it possible to use high strength reinforcing steel (Grade 600 or higher) in RC columns.

Table 4. *Maximum strength of confined concrete*

	Unconfined	Confined	
	$f_{y,\varepsilon2}$	σ_2/f_{ck}	$f_{y,\varepsilon2,c}$
≤ C50/60	460	≥0.029	600
C55/67	506	≥0.018	600
C60/75	529	≥0.014	600
C70/85	552	≥0.009	600
C80/95	575	≥0.005	600
C90/105	598	≥0.001	600

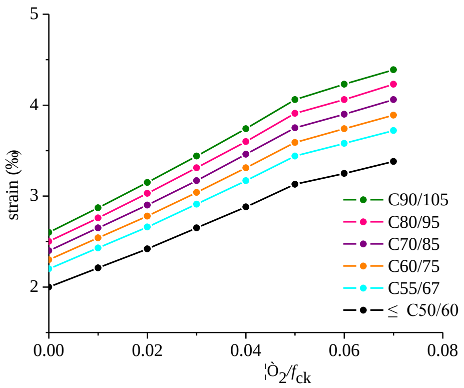

Figure 16. Increased strain of confined concrete

4.4 Construction Practice on Steel Reinforcing Bar

Use of Grade 600 or higher strength steel reinforcing bar is expected to bring higher productivity and saving in many aspects of construction. Therefore, it is common to use Grade 600 or higher strength steel rebar (up to USD685) in high-rise residential and commercial buildings construction in Japan. Hoops up to SBPD1275 are being used for columns in Japan. One reason for using ultra-high strength hoops in columns is to generate confinement of concrete. As mentioned above, EC2 allows the use of confinement of concrete to increase the effective stress-strain relationship of concrete using adequately designed hoops. With the increased strain of confined concrete, it is possible to use high strength compression reinforcement (Grade 600 or higher) in RC columns to resist axial loading. However, links are not used to enhance and improve concrete in Singapore. There is a need to educate our engineers in order to take advantage of high strength reinforcing bars for column design.

Accompanied with the use of high strength reinforcing bar, mechanical joints (threaded-rebar joint and mortar-grouted joint, as shown in Figure 17 are used extensively in prefabrication instead of normal lapping joint to achieve the goal of better productivity of the reinforcing bar cage construction work in Japan. This is because it is easier to install and fit reinforcing bar cages. There is sufficient space to allow for some lack of fit. Use of mechanical joints in construction can bring higher productivity and saving in many aspects of construction: less steel reinforcement is needed (up to 20% reduction); less workers are needed in steel reinforcement fabrication; less space is required for storage of steel reinforcement and up to 50% time reduction can be accomplished. Additionally, it encourages the adoption of pre-cast system in high-rise residential construction. By using precast members (PC beams, PC columns and PC slabs. manufactured in precast factories for high-rise buildings, esp. condominiums, it is possible to increase workability at limited site area, shorten construction period and achieve excellent cost performance.

(a) Threaded-rebar joint

(b) Mortar-grouted joint

(c) Prefabrication

Figure 17. Mechanical joints used for prefabrication

5. HIGH STRENGTH COMPOSITE STEEL

High strength construction materials are now attractive owing to their economic and architectural advantages. However, material brittleness could be one of the problems for high strength concrete and local buckling may be a problem for high strength steel. To overcome these problems, one solution is to use composite structures, especially composite columns where the ductility of the concrete can be enhanced by the effect of steel and the local buckling of the steel can be prevented by the concrete.

Although composite columns exhibit better ductility and higher buckling resistance compared to steel columns and reinforced concrete columns, EC4 gives narrower range of material strength for steel and concrete compared to EC2 and EC3. EC4 applies to composite columns with steel Grades S235 to S460 and concrete of strength classes C20/25 to C50/60. EC4 should be extended to cater for higher strength concrete and steel. However, material compatibility between steel Grade and concrete class should be observed.

For composite columns under axial compression, it is necessary to ensure that the yielding of the steel section occurs before the concrete reaches its maximum compression strain. It means that the selected steel should reach its yield strength at the maximum compression strain of concrete. The yield strength of steel may be calculated according to EN 1993-1-1 with elastic modulus E_a= 210GPa. The maximum compression strain of concrete under axial compression is ε_{c2} assumed that the parabola-rectangle diagram is used.

Table 4 shows the maximum strength of steel that can be developed at the compression strain ε_{c2} of concrete. It can be found that for steel Grade above S500 the full strength of steel is not available for composite column to resist axial compression. For S460 steel, it may be used with concrete class equal or above C55/67 and for S500 steel, it may be used with concrete class not below C70/85. It is noted that the strain of concrete ignores the confinement effect from steel. If the increase of strain by confinement is taken into account, higher steel Grade could be used.

Table 4. ***Maximum strength of steel at compression strain ε_{c2}***

Grade	S235	S275	S355	S420	S460	S500	S550	S620	S690
≤ C50/60	235	275	355	420	420	420	420	420	420
C55/67	235	275	355	420	460	464	464	464	464
C60/75	235	275	355	420	460	483	483	483	483
C70/85	235	275	355	420	460	500	504	504	504
C80/95	235	275	355	420	460	500	525	525	525
C90/105	235	275	355	420	460	500	546	546	546
$f_{y,\varepsilon_2} = E_a \varepsilon_{c2} \le f_y$									

6. CONCLUSIONS

This paper discussed the possibility of extending the use of emerging high performance and HSS in construction to improve productivity. Highlights are given to the tensile behavior of T-stub joints made of high strength structural steel including RQT HSS in Grade S690 and TMCP steel in Grade S385 and S440, and the issues of using high strength Grade 600 reinforcing steel bars and high strength steel in composite columns. It is concluded that HSS may behave quite differently from traditional NSS in certain aspects but HSS have great potential for future practical applications.

7. ACKNOWLEDGEMENT

This research is supported by Singapore Ministry of National Development (MND) Research Fund on Sustainable Urban Living (Grant No. MNDRF SUL2013-4). Any opinions, findings and conclusions expressed in this paper are solely those of the authors and do not necessarily reflect the view of grant awarding agency.

8. REFERENCES

AISC (2005). Specification for structural steel buldings. ANSI/AISC 306-05. Chicago, Americal Institute of Steel Construction.

Al-Khatab, Z. and A. Bouchaïr (2007). "Analysis of a bolted T-stub strengthened by backing-plates with regard to Eurocode 3." Journal of Constructional Steel Research 63(12): 1603-1615.

AWS (2008). Structural Welding Code. steel. Miami, American National Standards Institue.

Bai, Q. and Y. Bai (2014). 31 - Use of High-Strength Pipeline Steel. Subsea Pipeline Design, Analysis, and Installation. Q. Bai and Y. Bai. Boston, Gulf Professional Publishing: 675-694.

Bhadeshia, H. K. D. H. and R. W. K. Honeycombe (2006). Steel: microstructure and properties. Oxford, United Kingdom, Elsevier Science & Technology.

Bjorhovde, R. (2004). "Development and use of high performance steel." Journal of Constructional Steel Research 60(3–5): 393-400.

BSI (2004). Design of Concrete Structures - Part 1-1: General Rules and Rules for Buildings. London, British Standards Institution.

BSI (2004). Hot Rolled Products of Structural Steel: Part 4 Technical Delivery Conditions for Thermalmechanical Rolled Weldable Fine Grain Structural Steel, BS EN 10025-4. London, British Standards Institution.

BSI (2004). hot rolled products of structural steel: part 6 technical delivery conditions for flat products of high yield strength structural steel in the quenched and tempered condition, BS EN 10025-6. London, British Standards Institution.

BSI (2005). Eurocode 3: design of steel structures: part 1-1 general rules and rules for buildings, BS EN 1993-1-1. London, British Standard Institution.

BSI (2005). Eurocode 3: design of steel structures: part 1-8 design of joints, BS EN 1993-1-8. London, British Standard Institution.

Chen, J. and B. Young (2006). "Behavior of High strength structural steel at elevated temperatures." Journal of structural eninggering: P1948-1954.

Chiew, S. P., M. S. Zhao, et al. (2014). "Mechanical properties of heat-treated high strength steel under fire/post-fire conditions." Journal of Constructional Steel Research 98(0): 12-19.

Girão Coelho, A. M. and F. S. K. Bijlaard (2007). "Experimental behaviour of high strength steel end-plate connections." Journal of Constructional Steel Research 63(9): 1228-1240.

Han, L.-H., C.-C. Hou, et al. (2014). "Behaviour of high-strength concrete filled steel tubes under transverse impact loading." Journal of Constructional Steel Research 92: 25-39.

Hasegawa, T., Y. Tomita, et al. (1998). "Influence of tantalum and nitrogen contents, normalizing condition and TMCP process on the mechanical properties of low-activation 9Cr–2W–0.2V–Ta steel for fusion application." Journal of Nuclear Materials 258–263, Part 2: 1153-1157.

Healy, J. and J. Billingham (1995). "Metallurgical considerations of the high yield to ultimate ratio in high strength steel for use in offshore engineering." 14th International Conference of OMAE III:365.

Mohandas, T., G. Madhusudan Reddy, et al. (1999). "Heat-affected zone softening in high-strength low-alloy steel." Journal of Materials Processing Technology 88(1–3): 284-294.

Nakano, Y., Y. Saito, et al. (1988). A 460MPa YIELD STRENGTH STEEL PLATE PRODUCED BY TMCP FOR ARCTIC USE. Proceedings of the Metallurgical Society of the Canadian Institute of Mining and Metallurgy. G. E. R. F. Crawley. Oxford, Pergamon: 221-233.

Pocock, G. (2006). "High strength steel use in Australia, Japan and the US." Structural Engineer 84(21): 27-30.

Pocock, G. (2006). "High Strength Steel Use in Australia, Japan and the US." The Structural Engineer Vol.84(21): pp. 27-30.

Qiang, X., F. Bijlaard, et al. (2012). "Dependence of mechanical properties of high strength steel S690 on elevated temperatures." Construction and Building Materials 30(0): 73-79.

Qiang, X., F. S. K. Bijlaard, et al. (2012). "Deterioration of mechanical properties of high strength structural steel S460N under transient state fire condition." Materials & Design 40(0): 521-527.

Shi, G., H. Ban, et al. (2012). "Tests and numerical study of ultra-high strength steel columns with end restraints." Journal of Constructional Steel Research 70(0): 236-247.

Tensi, H. M., A. Stich, et al., Eds. (2007). Chapter 9: quenching and quenching techonology. Steel heat treatment handbook: metallurgy and technology, Taylor & Francis.

Uy, B. (2008). "Stability and ductility of high performance steel sections with concrete infill." Journal of Constructional Steel Research 64(7–8): 748-754.

Wang, K. and B. Young (2013). "Fire resistance of concrete-filled high strength steel tubular columns." Thin-Walled Structures 71: 46-56.

Yorgun, C. and G. Bayramoglu (2001). "Cyclic tests for welded-plate sections with end-plate connections." Journal of Constructional Steel Research 57: 1309-1320.

Zhao, X.-L., D. Van Binh, et al. (2004). "Stub column tests of fabricated square and triangular sections utilizing very high strength steel tubes." Journal of Constructional Steel Research 60(11): 1637-1661.